

On the Formation of the Popcorn Flavorant 2,3-Butanedione (CH₃COCOCH₃) in Acetaldehyde-Containing Interstellar ices

N. Fabian Kleimeier,^[a] Andrew M. Turner,^[a] Ryan C. Fortenberry^[b], and Ralf I. Kaiser^{*[a]}

[a] Dr. N. F. Kleimeier, Dr. A. M. Turner, Prof. Dr. R. I. Kaiser
Department of Chemistry and W. M. Keck Research Laboratory in Astrochemistry
University of Hawai'i at Manoa
2545 McCarthy Mall, Honolulu, HI 96822 (USA)
E-mail: ralfk@hawaii.edu

[b] Prof. Dr. R. C. Fortenberry
Department of Chemistry & Biochemistry
University of Mississippi
322 Coulter Hall, University, MS 38677-1848 (USA)

Supporting information for this article is given via a link at the end of the document.

Abstract: Acetaldehyde (CH₃CHO) is ubiquitous throughout the interstellar medium and has been observed in cold molecular clouds, star forming regions, and in meteorites such as Murchison. As the simplest methyl-bearing aldehyde, acetaldehyde constitutes a critical precursor to prebiotic molecules such as the sugar deoxyribose and amino acids via the Strecker synthesis. In this study, we reveal the first laboratory detection of 2,3-butanedione (diacetyl, CH₃COCOCH₃)—a butter and popcorn flavorant—synthesized within acetaldehyde-based interstellar analog ices exposed to ionizing radiation at 5 K. Detailed isotopic substitution experiments combined with tunable vacuum ultraviolet (VUV) photoionization of the subliming molecules demonstrate that 2,3-butanedione is formed predominantly via the barrier-less radical-radical reaction of two acetyl radicals (CH₃ĊO). These processes are of fundamental importance for a detailed understanding of how complex organic molecules (COMs) are synthesized in deep space thus constraining the molecular structures and complexity of molecules forming in extraterrestrial ices containing acetaldehyde through a vigorous galactic cosmic ray driven non-equilibrium chemistry.

Introduction

To date, more than 200 molecules ranging from molecular hydrogen (H₂) up to fullerenes (C₆₀, C₇₀) have been detected in circumstellar and interstellar environments.^[1] Complex organic molecules (COMs)—usually defined by the astronomical community as carbon-bearing organics comprised of six or more atoms, mostly carbon, oxygen, and/or nitrogen at various degrees of hydrogenation—represent a key class of interstellar molecules and main contributor to the cosmic carbon budget since they account for nearly one third of all detected molecules in extraterrestrial environments.^[2] Laboratory simulation experiments along with astronomical observations suggest that the majority of these organics are synthesized in cold molecular clouds—opaque environments with gas phase number densities

of 10⁴ to 10⁶ molecules cm⁻³ and nanometer-sized, ice-coated dust particles.^[3] The opaqueness of these molecular clouds results in average temperatures of the dust particles as low as 10 K. Considering the low temperature, gas-phase molecules and atoms accrete on these silicate- and carbon-bearing dust particles resulting in the aggregation of several hundred nanometer thick ices.^[4] Water (H₂O), carbon monoxide (CO), carbon dioxide (CO₂), methanol (CH₃OH), methane (CH₄), ammonia (NH₃), and formaldehyde (H₂CO) represent the main constituents of these ices.^[4,5]

Through interaction with the internal ultraviolet (UV) field generated even within dense molecular clouds^[6] and by energetic galactic cosmic ray particles (GCRs), energies of up to 0.3–3.0 eV per molecule are deposited on average into each molecule within the ices over typical life times of these clouds of 10⁶–10⁷ years.^[7] This energy deposition initiates chemical bond breaking processes and the synthesis of new molecules via non-equilibrium processes such as amino acids,^[8–11] dipeptides,^[12] astrobiologically important phosphorus bearing molecules like (di)phosphates^[13] and alkylphosphonic acids,^[14] along with sugar-related molecules such as glycolaldehyde (HCOCH₂OH).^[15] One key class of the organics detected are carbonyl-bearing (–C=O) species including molecules with an aldehyde group (–CHO) (Fig. 1) as they constitute key building blocks of prebiotic molecules as for example sugars^[16] and amino acids^[17,18] along with their precursors methanol^[19] and acetic acid.^[20] Eventually, at the end of their lifetimes, molecular clouds undergo gravitational collapse, new stars form, and molecules synthesized on the dust particles are incorporated at least partially into planetary systems along with asteroids and comets, which can then deliver organics to planets such as proto-Earth.^[3,21,22]

Acetaldehyde (CH₃CHO) in particular has emerged as a critical precursor to biologically relevant molecules: the sugar 2-

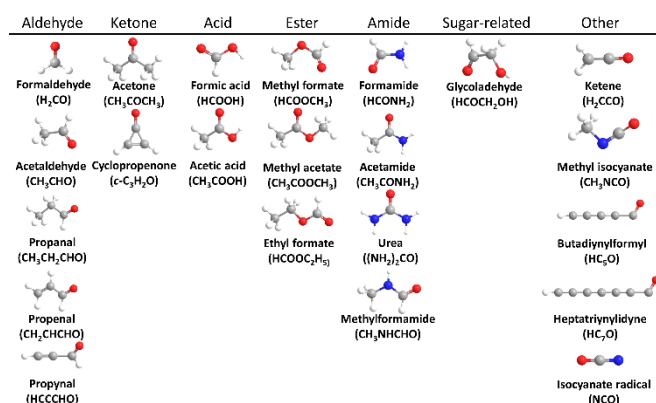


Figure 1. Selected carbonyl-bearing complex organic molecules (COMs) detected in the interstellar medium (ISM).

deoxyribose ($\text{HCOCH}_2(\text{CHOH})_3\text{H}$) may form via the reaction of acetaldehyde with glyceraldehyde ($\text{H}_2\text{COHCHOHCHO}$), which in turn can be synthesized from formaldehyde (H_2CO) and glycolaldehyde (HCOCH_2OH).^{[23],[24]} Laboratory experiments provide compelling evidence that acetaldehyde can easily form in interstellar ices containing carbon monoxide and methane,^[25–28] methanol,^[29] ethane (CH_3CH_3) or ethylene (CH_2CH_2),^[30] pure methanol ices,^[31] or by oxidation of ethanol ($\text{CH}_3\text{CH}_2\text{OH}$)^[32]/2-propanol ($\text{CH}_3\text{CH}_2\text{OHCH}_3$)^[33] exposed to ionizing radiation. Considering the facile formation of acetaldehyde in interstellar and solar system analog ices, it is not surprising that the acetaldehyde molecule has been detected throughout the interstellar medium: in cold molecular clouds such as TMC-1, in warmer envelopes around star-forming regions, e.g., Sgr B2^[34,35], towards hot cores such as NGC 6334F,^[36] quiescent regions like CB 17,^[37] in meteorites like Murchison,^[38] comets such as Hale-Bopp^[39] and during the Rosetta mission on 67P/Churyumov-Gerasimenko.^[40] Furthermore, tentative detections of acetaldehyde in interstellar ices have been published with upper limits of 3%^[41,42] and 10%^[5] relative to water.

However, despite the fundamental importance of acetaldehyde as a precursor to biologically relevant, complex organic molecules in extraterrestrial ices, the underlying low-temperature and radiation chemistry of acetaldehyde on interstellar and solar system analog ices is still elusive as research has focused predominantly on gas phase reactions, both experimentally and computationally, during the last decades, especially as a model compound for roaming processes.^[43] In pyrolysis studies 796 K, the main radicals formed are methyl ($\dot{\text{C}}\text{H}_3$) and formyl ($\text{H}\dot{\text{C}}\text{O}$) via simple carbon-carbon bond cleavage. Furthermore, the acetyl radical ($\text{CH}_3\dot{\text{C}}\text{O}$) is subsequently generated by hydrogen abstraction initiated by atomic hydrogen.^[44] Under these conditions, the formyl radical rapidly decomposes into atomic hydrogen and carbon monoxide, whereas methyl and acetyl radicals react to form ethane and

acetone (CH_3COCH_3). At higher temperatures (1000–1900 K), additional products are observed, including vinyl alcohol (CH_2CHOH), water, and acetylene (HCCH)^[45] as well as methane and carbon monoxide through hydrogen roaming pathways and/or via a tight transition state.^[46,47]

Further, gas phase photolysis studies reveal a strong dependence of the products and reaction pathways on the photon energy. At wavelengths around 308 nm, formyl, methyl and acetyl are the main radicals formed.^[48] Furthermore, carbon monoxide and methane form predominantly by methyl radical roaming, but also from hydrogen atom roaming.^[49–51] In the photolysis of acetaldehyde cations between 316 and 228 nm, cations of the same molecules were observed: $\text{C}_2\text{H}_3\text{O}^+$, HCO^+ , CH_3^+ , and CH_4^+ .^[52] Triple fragmentation to yield carbon monoxide, atomic hydrogen and methyl was observed as an additional channel at 248 nm.^[53] Neither ketene (H_2CCO) nor acetyl (CH_3CO) were found to be a significant intermediate to the formation of carbon monoxide in the acetaldehyde photolysis.^[54] In gas phase photolysis studies at 205 nm, however, both vinoxy and acetyl radicals were detected at a ratio of 2 : 1.^[55] Ketene was first detected as a product in gas phase photolysis experiments conducted at 157 nm, where its formation with molecular hydrogen constitutes a major reaction channel alongside acetyl and atomic hydrogen, formyl and methyl, methylene (CH_2) and formaldehyde, vinyl (C_2H_3) and hydroxy (OH) radicals, and acetylene plus water.^[56] Recently, Harrison *et al.* also revealed ketene as a major product in photolysis experiments conducted at 305.6 nm and confirmed that this molecule forms alongside molecular hydrogen from acetaldehyde molecules.^[57]

In the solid phase, only limited studies were conducted. Irradiation of acetaldehyde at 25–35 K with low energy electrons (15.5 eV) yielded methane (CH_4), carbon monoxide (CO), and propionaldehyde ($\text{CH}_3\text{CH}_2\text{CHO}$) indicating that vinoxy ($\dot{\text{C}}\text{H}_2\text{CHO}$), but likely no acetyl radicals ($\text{CH}_3\dot{\text{C}}\text{O}$), are formed or that the acetyl radicals immediately dissociate into methyl and carbon monoxide.^[58] On the other hand, electron spin resonance (ESR) studies of solid acetaldehyde in noble gas matrices at 77 K exposed to high energy electrons (1 MeV) revealed acetyl ($\text{CH}_3\dot{\text{C}}\text{O}$) to be the dominating radical.^[59] This was supported by another ESR study of acetaldehyde isolated in freon matrices after irradiation with γ -radiation. These experiments showed that acetaldehyde cations formed during the irradiation undergo charge neutralization and convert into either acetyl or 1-hydroxyethyl ($\text{CH}_3\dot{\text{C}}\text{HOH}$) radicals.^[60] An extended study processing acetaldehyde ices at 77 K with either X- or γ -rays revealed that solid acetaldehyde polymerizes primarily by (unknown) radicals “R” connecting to acetaldehyde to form

ARTICLE

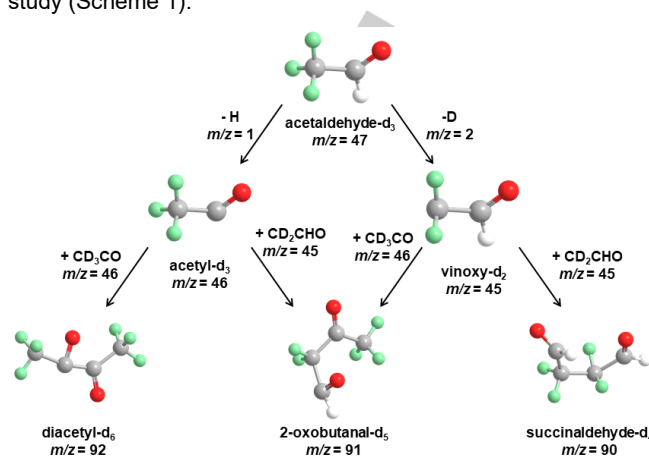
CH_3CHOR , which can then react with acetaldehyde molecules to form long polymer-like chains.^[61] Furthermore, hydrogen atom bombardment of solid acetaldehyde was found to produce methane, methanol, formaldehyde, and possibly ethanol.^[62] Recently, Hudson and Ferrante suggested that irradiation of acetaldehyde with 0.8 MeV protons leads to the formation of the acetyl and vinoxy radicals along with ketene, carbon monoxide and methane, however, complex organics could not be identified due to the overlap of their infrared modes with those of acetaldehyde.^[63]

In this study, we demonstrate that 2,3-butanedione (diacetyl, $\text{CH}_3\text{COCOCH}_3$)—a butter flavorant exploited in artificial butter flavor for popcorn—is synthesized within acetaldehyde-based interstellar analog ices exposed to ionizing radiation at 5 K by exploiting vacuum ultraviolet (VUV) photo ionization (PI) of the subliming products coupled with a reflectron time-of-flight mass spectrometer (ReToF-MS). The laboratory identification of 2,3-butanedione—a vicinal diketone carrying two adjacent C=O groups—delivers persuasive evidence that chemically complex organics carrying two carbonyl moieties can be synthesized easily in acetaldehyde-doped interstellar and solar system ices at temperatures as low as 10 K predominantly via the recombination of two acetyl radicals ($\text{CH}_3\dot{\text{C}}\text{O}$). Although complex organics carrying two oxygen-bearing functional groups such as ethylene glycol ($\text{HOCH}_2\text{CH}_2\text{OH}$), methoxymethanol ($\text{CH}_3\text{OCH}_2\text{OH}$), and glycolaldehyde (HCOCH_2OH) have been detected in the interstellar medium (Figure 1), diketones are still elusive; their astronomical detection would expand our understanding of the radiation-induced low temperature chemistry within interstellar ices and could define the inventory of radicals and successive radical-radical reactions followed by the decomposition of precursors to complex organics in deep space.

Results and Discussion

The experiments were carried out in an ultrahigh-vacuum (UHV) surface-science chamber at pressures of a few 10^{-11} Torr.^[64] In separate experiments, ices of acetaldehyde (CH_3CHO) and acetaldehyde-2,2,2- d_3 (CD_3CHO) were prepared by condensing gaseous acetaldehyde or acetaldehyde-2,2,2- d_3 onto a polished silver wafer at 5 K. After the deposition, the ices were subjected to energetic electrons at doses from 0.31 ± 0.06 to 1.2 ± 0.2 eV molecule⁻¹ simulating the energy deposited in interstellar ices by secondary electrons generated by galactic cosmic rays (GCRs) penetrating the ices over lifetimes of molecular clouds of a few 10^6 years (Table S1).^[25] The exploitation of partially isotopically labeled reactants permits the assignments

of distinct mass-to-charge (m/z) ratios that do not overlap with other COMs to be correlated with the isomers of interest in this study (Scheme 1).



Scheme 1. Interaction of acetaldehyde-2,2,2- d_3 with energetic electrons can lead to the formation of the acetyl and the vinoxy radical by removal of a deuterium or hydrogen atom, respectively. The vinoxy radical can react with another vinoxy radical to form succinaldehyde ($m/z = 90$) or with an acetyl radical to form 3-oxobutanal ($m/z = 91$). Diacetyl ($m/z = 92$) can form from the reaction of two acetyl radicals.

After irradiation, the sample was heated at 0.5 K min^{-1} to 320 K (Temperature Programmed Desorption, TPD) to sublime the reactant and product molecules. Changes in the ice during irradiation and warm up were monitored *on line* and *in situ* by Fourier Transform Infrared Spectroscopy (FTIR) to observe the emergence of spectral features of newly formed smaller molecules along with functional groups during irradiation as well as changes in these patterns upon heating. As COMs often have similar infrared absorptions, infrared spectroscopy rarely allows the unambiguous detection of discrete molecules due to overlapping absorptions.^[65] Therefore, the subliming molecules were also photoionized (PI) by tunable vacuum ultraviolet (VUV) light and detected according to their m/z ratios in a reflectron time-of-flight mass spectrometer (ReToF-MS). By systematically tuning the photon energy, distinct structural isomers of the products can be exclusively distinguished.^[64] Note that these interstellar model ices containing acetaldehyde were chosen to explore the proof of concept that COMs carrying (methyl-) carbonyl moieties can be synthesized through energetic processing by ionizing radiation. Considering that carbon monoxide (CO) and methane (CH_4) were both observed in interstellar ices by the Spitzer space telescope toward low-mass star-forming regions^[66] and laboratory experiments revealed explicitly the formation of acetaldehyde in carbon monoxide-methane ices,^[25–27] although not unambiguously detected, acetaldehyde is expected to be present in interstellar ices. Acetaldehyde was suggested as a potential carrier of the

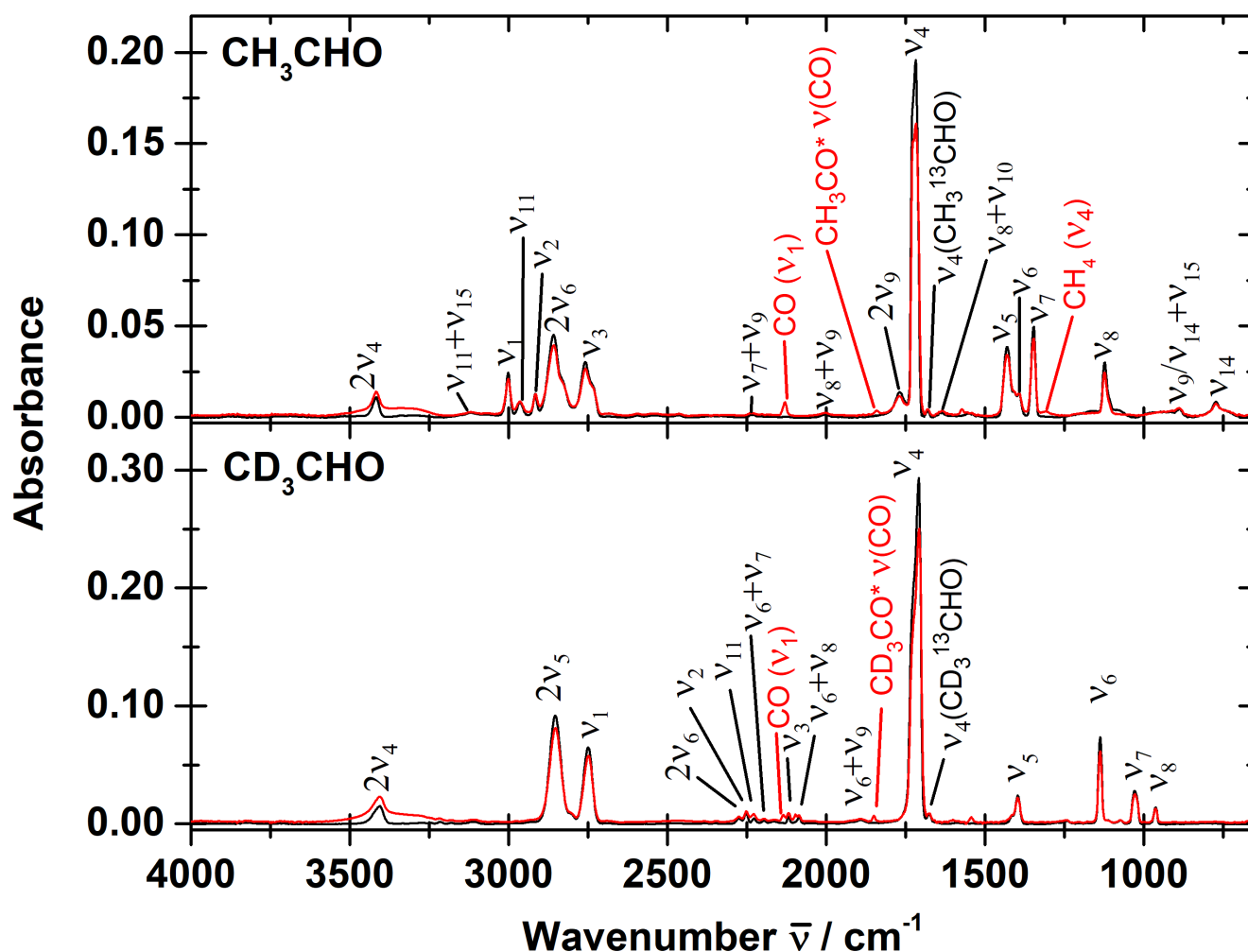


Figure 2. FTIR spectra of acetaldehyde (top) and acetaldehyde-2,2,2-d₃ (bottom) before (black) and after irradiation (red). To enhance the visibility of small peaks arising after irradiation, the spectra have been offset by 0.001.

1350 cm⁻¹ (7.41 μm) band observed toward W 33A,^[42] but this proposition requires confirmation in follow-up observations.

Figure 2 depicts the spectra of both acetaldehyde and acetaldehyde-2,2,2-d₃ ices before and after the electron bombardment with a dose of 1.2 eV molecule⁻¹. The absorptions in the unirradiated ice can be attributed to distinct vibrational modes of acetaldehyde ices such as the stretching mode of the carbonyl moiety (ν_4) at 1718–1926 cm⁻¹ (Tables S2 and S3, Supporting Information). As a result of the irradiation, the decrease in absorbance of all peaks associated with acetaldehyde is apparent revealing that $18 \pm 3\%$ and $11 \pm 2\%$ of acetaldehyde and acetaldehyde-2,2,2-d₃, respectively, was transformed to new molecules. The formation of these molecules is evident from several new infrared features in the irradiated acetaldehyde ice emerging at 3550–3200 cm⁻¹, 2140 cm⁻¹, and 1300 cm⁻¹. These can be linked to OH stretching modes, an overlap

of the CO stretch of both carbon monoxide and ketene, and the deformation of methane, respectively, as degradation products of acetaldehyde.^[67] These conclusions are supported by the FTIR spectra of the acetaldehyde-2,2,2-d₃ ice. Here, new absorption features are emerging at 3550–3200 cm⁻¹, 2140 cm⁻¹, and 2098 cm⁻¹, which can be assigned to OH stretching, the CO stretch of carbon monoxide, and the CO stretch of ketene-d₂ (CD₂CO).^[68] Most important, the acetyl radical (CH₃ĊO) can be identified at 1841 cm⁻¹ (Fig. 3) in the irradiated acetaldehyde ice, whereas the acetyl-d₃ is detected at 1852 cm⁻¹ in the irradiated acetaldehyde-2,2,2-d₃ ice. Both absorptions are in good agreement with measurements of the acetyl radical in an argon matrix by Jacox, who identified the acetyl radical at 1842 cm⁻¹ and the acetyl-d₃ radical at 1855 cm⁻¹.^[69]

Furthermore, absorptions are detected at 1571 cm⁻¹ and 1540 cm⁻¹ in the irradiated acetaldehyde and acetaldehyde-2,2,2-

d_3 ice. Hudson and Ferrante assigned an absorption at 1572 cm^{-1} to the vinoxy radical ($\dot{\text{C}}\text{H}_2\text{CHO}$),^[63] however, Jacox reported the absorptions of vinoxy at 1525 cm^{-1} and 1541 cm^{-1} and those of vinoxy- d_2 ($\dot{\text{C}}\text{D}_2\text{CHO}$) at 1534 cm^{-1} and 1537 cm^{-1} (indicated by grey lines in Fig. 3).^[69] Although the position of the absorption in the acetaldehyde-2,2,2- d_3 ice is in reasonable agreement with the values by Jacox and the absorption in the acetaldehyde ice is in good agreement with the value reported by Hudson and Ferrante, the isotopic shift of 31 cm^{-1} is too large for this assignment to be correct as shifts reported by Jacox for the vinoxy- d_2 radical amounted to only 9 cm^{-1} and 4 cm^{-1} with respect to vinoxy.^[69]

The intensities of this peak and the one associated with the acetyl radical decrease rapidly upon warming of the irradiated samples once temperatures reach around 40 K . As seen in Fig. S1, the peak around 1550 cm^{-1} vanishes completely at around 60 K , whereas the acetyl peak can be seen up to temperatures of 90 K . This suggests that both peaks are linked to radicals (or thermally labile closed shell species) that degrade or react with other molecules/radicals once their mobility in the ice is sufficient. However, the isotopic shift of 31 cm^{-1} found in this study between the CH_3CHO and CD_3CHO ice is too large for this assignment as Jacox *et al.* measured shifts of 12 cm^{-1} and 7 cm^{-1} for the two CCO absorptions they found in the matrix isolation study of the same isotopologues.^[69]

Most important, since the fundamentals of functional groups such as of carbonyls in COMs potentially synthesized during the radiation processing of acetaldehyde often fall in the same range, infrared spectroscopy rarely allows an identification of individual COMs.^[63,70] Therefore, an alternative analytical technique is critical to probe discrete organics in the irradiated ices. This goal is accomplished by exploiting PI-ReToF-MS (Figs. 4–6) during the temperature programmed desorption (TPD) phase of the irradiated ices. Considering the infrared spectroscopic detection of the acetyl- d_3 radical ($\text{CD}_3\dot{\text{C}}\text{O}$), the PI-ReToF-MS studies are also aimed in the elucidation of potential reaction mechanisms. Here, partly deuterated acetaldehyde-2,2,2- d_3 (CD_3CHO ; $m/z = 47$) can lose a hydrogen or deuterium atom from the methyl and formyl group, respectively, upon exposure to ionizing radiation (Scheme 1). This would lead to acetyl- d_3 radical ($\text{CD}_3\dot{\text{C}}\text{O}$, $m/z = 46$) and to the vinoxy-2,2- d_2 radical ($\dot{\text{C}}\text{D}_2\text{CHO}$ $m/z = 45$), respectively. Radical-radical recombination can therefore form three distinct structural isomers: diacetyl- d_6 ($m/z = 92$; recombination of two acetyl- d_3 radicals), 2-oxobutanol- d_5 ($m/z = 91$; recombination of one vinoxy-2,2- d_2 and one acetyl- d_3 radical), and succinaldehyde- d_4 ($m/z = 92$; recombination of two vinoxy-2,2- d_2 radicals).

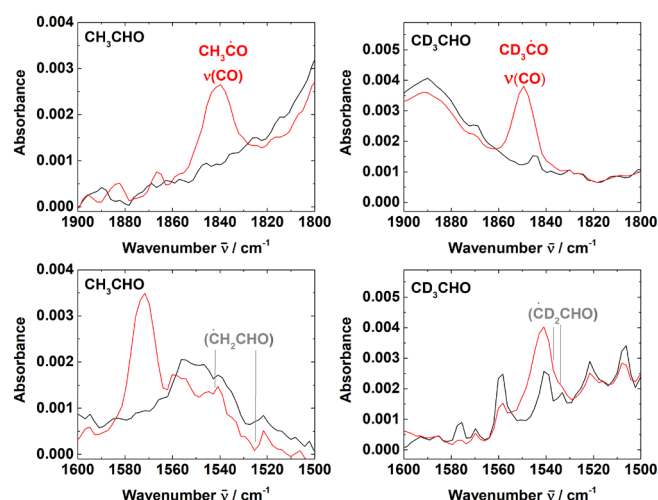


Figure 3. IR spectrum in the region of the acetyl radical (top) and the vinoxy radical (bottom) before (black) and after irradiation (red). The grey labels in the bottom graphs denote reported energies of the CCO stretch of the vinoxy radical in a solid argon matrix.^[69]

To elucidate the reaction product(s) formed, the studies were first conducted in separate experiments with acetaldehyde and acetaldehyde-2,2,2- d_3 ices at a photon energy of 10.49 eV to ionize the subliming molecules (Fig. 4, top left, Fig. S2). Compared to the non-irradiated samples (Fig. S3), several distinct peaks arise after irradiation with a dose of $0.31\text{ eV molecule}^{-1}$ (Table S4, supporting information). Furthermore, the ReToF-MS desorption profile of acetaldehyde changes drastically. After the irradiation, it sublimes from its nominal sublimation onset at 90 K (non-irradiated sample) up to 320 K , i.e. the maximum temperature exploited in the TPD phase. This indicates a polymerization of the acetaldehyde, either due to radical reactions with acetaldehyde as studied by Chaechaty and Marx after irradiation of acetaldehyde ice with X- and γ -rays, or ionic reactions as concluded as main reaction pathway by A. Charlesby.^[61,71] Most important, ion counts connected to $\text{C}_4\text{D}_6\text{O}_2$ ($m/z = 92$), $\text{C}_4\text{D}_5\text{HO}_2$ ($m/z = 91$), and $\text{C}_4\text{D}_4\text{H}_2\text{O}_2$ ($m/z = 90$) are detected in the TPD traces and exhibit the same TPD profile as $\text{C}_4\text{H}_6\text{O}_2$ ($m/z = 86$) and $\text{C}_4\text{D}_6\text{O}_2$ ($m/z = 92$) in irradiated acetaldehyde and acetaldehyde- d_4 ices, respectively (Fig. 5), confirming the assumed empirical formula. Considering the calculated adiabatic ionization energies (*IE*; Tabs. S5 – S7), ion counts at these mass-to-charge ratios could correspond to *all* products of acetyl and vinoxy radical-radical recombination, i.e. diacetyl- d_6 , 2-oxobutanol- d_5 , and succinaldehyde- d_4 (Scheme 1) including their (di)enol tautomers. Therefore, additional PI-ReToF-MS experiments were conducted exploiting photon energies of 10.11 eV , 9.50 eV , 9.30 eV , and 9.10 eV to discriminate the isomer(s) formed. These photon energies in combination with the isotopic labeling of the acetaldehyde-2,2,2-

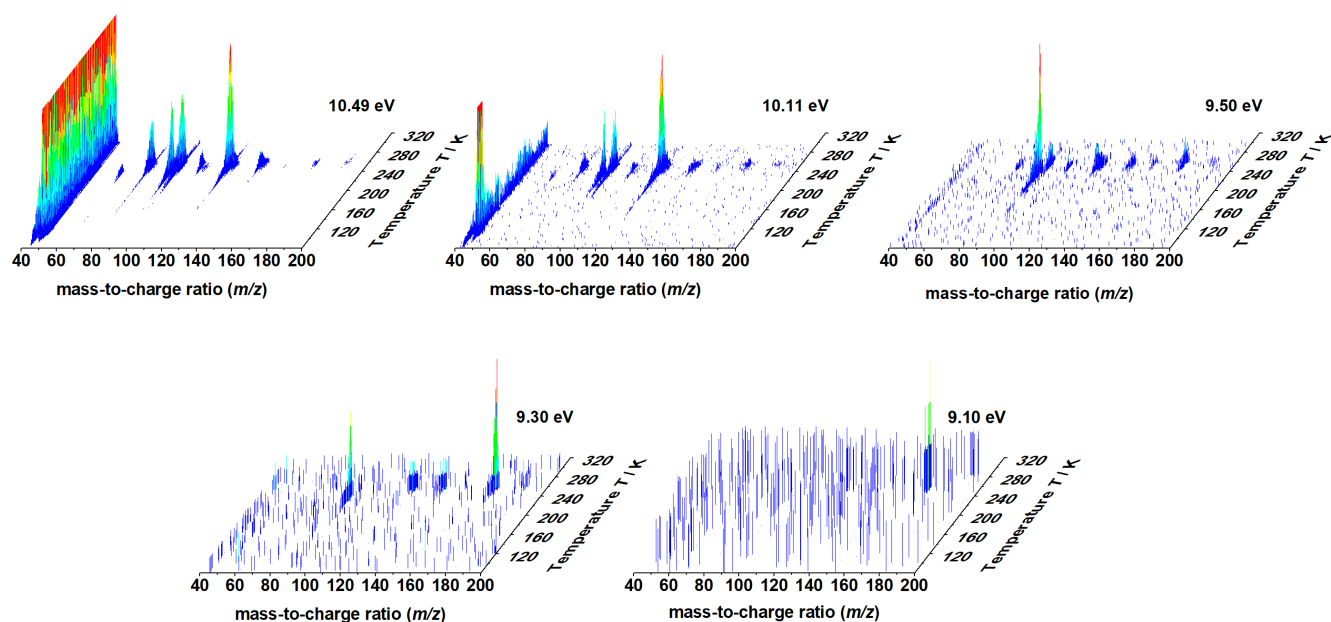


Figure 4. Temperature-dependent PI-ReToF mass spectra of subliming reactants and products in irradiated acetaldehyde-2,2,2- d_3 ices recorded at different photon energies. The graphs have been scaled to the height of the highest product peak.

d_3 allow for *unambiguous* identification of all possible isomers at the aforementioned mass-to-charge ratios based on the following strategy.

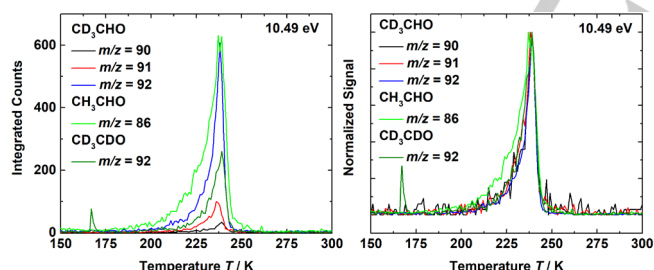


Figure 5. Temperature programmed desorption profiles of mass-to-charge ratios corresponding to $C_4D_4H_2O_2$ ($m/z = 90$), $C_4D_3HO_2$ ($m/z = 91$), and $C_4D_5O_2$ ($m/z = 92$) in irradiated acetaldehyde- d_3 ice. For comparisons, $C_4H_6O_2$ ($m/z = 86$) in irradiated acetaldehyde ice and $C_4D_5O_2$ ($m/z = 92$) in irradiated acetaldehyde- d_4 ice are also shown. Profiles were recorded at a photon energy of 10.49 eV. Left: raw data, right: normalized data.

At $m/z = 92$ (Table S5), the three highest photon energies (10.49 eV, 10.11 eV, 9.50 eV) ionize all isomers. Experiments conducted at 9.30 eV exclude the *cis* and *trans* isomer of 3-hydroxybut-3-en-2-one ($IE = 9.40$ eV and 9.39 eV, respectively); at 9.10 eV, diacetyl ($IE = 9.25$ eV) cannot be ionized leaving only buta-1,3-diene-2,3-diol ($IE = 8.95$ eV / 8.77 eV) as a possible isomer if a signal is still detected. Exploring possible reactions of one acetyl with one vinoxy radical leading to 2-oxobutanal- d_5 ($m/z = 91$, Table S6), photon energies of 10.49 eV and 10.11 eV can ionize all isomers with the exception of (*E*)-4-hydroxybut-3-en-2-one

($IE = 10.34$ eV) at 10.11 eV. Furthermore, data collected at 9.50 eV then exclude the (*Z*)-isomer ($IE = 9.98$ eV) and (*trans/cis*)-oxobutanal ($IE = 9.58$ / 9.96 eV); experiments at 9.30 eV exclude 3-hydroxybut-2-enal ($IE = 9.34$ eV). Signals detected at 9.10 eV can only be due to (*trans/cis*)-3-hydroxybut-3-enal ($IE = 9.23$ eV / 8.68 eV) and buta-1,2-diene-1,3-diol ($IE = 8.50$ eV), which could be distinguished at photon energies of 8.60 eV if necessary. Finally, reaction products resulting from the potential recombination of two vinoxy-2,2- d_2 radicals ($m/z = 90$, Table S7) can be ionized at 10.49 eV. Succinaldehyde ($IE = 10.19$ – 10.37 eV) can be excluded at 10.11 eV. Each of the TPD profiles of the previously discussed masses only exhibits a single peak (Figs. 5 and 6) suggesting that only one isomer is formed with each m/z ratio as desorption temperatures depend on the polarity of the molecules with more polar molecules desorbing later than less polar molecules. Furthermore, the desorption profiles are identical after scaling for all three m/z ratios (Fig. 5, right panel). The results obtained for $m/z = 92$, 91, and 90 at distinct photon energies are shown in Fig. 6. Considering the normalized TPD traces in the lower panel, it is evident that the shape of the sublimation profile does not change with different ionization energies. Since the TPD traces of $m/z = 92$ (Fig. 6) reveal only ion counts from 10.49 eV down to 9.3 eV and all TPD traces overlap after scaling, we can firmly identify the diacetyl- d_6 isomer contributing to ion counts at $m/z = 92$.

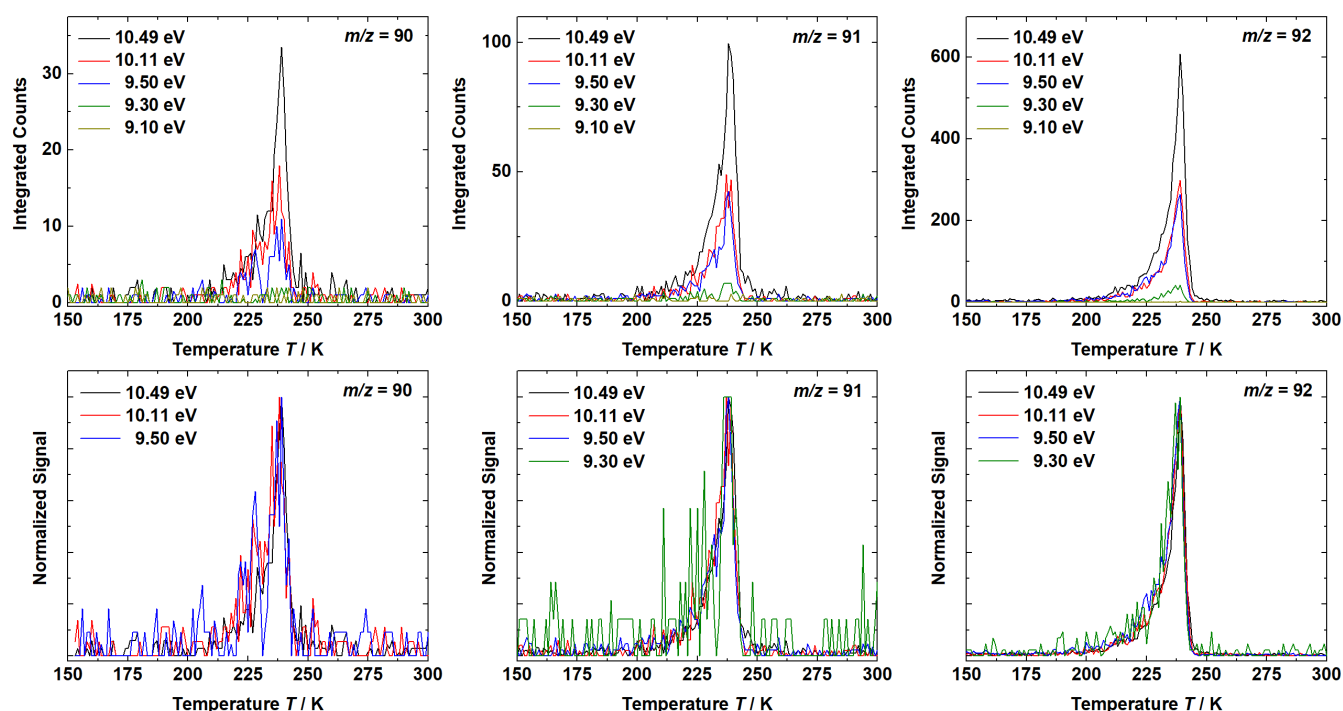


Figure 6. Temperature programmed desorption profiles of mass-to-charge ratios 90, 91, and 92 recorded at different photon energies. Top: raw data, bottom: normalized data.

Note that the shape of the profile remains the same (after scaling) for both $m/z = 92$ and 91 down to 9.30 eV and vanishes at 9.10 eV. The signal at $m/z = 90$ at 9.30 eV is expected to be below two counts (Fig. 6), which is too low to distinguish it from the background noise. Therefore, the identical TPD traces for each mass channel at various photon energy as discussed above suggest that a single isomer is formed with different deuteration levels.

This assignment is further confirmed by comparing the desorption profile of the detected molecule with that of diacetyl as shown in Fig. 7. Pure diacetyl deposited onto the silver surface exhibits two desorption peaks, a small one at $T = 135$ K and the major desorption peak at $T = 158$ K, far off the temperature seen in the irradiation experiments of acetaldehyde. However, when codepositing the diacetyl with acetaldehyde- d_4 and irradiating the sample using the same parameters as in the experiments presented here, most of the diacetyl gets trapped in the polymer matrix forming on the sample upon irradiation. The resulting TPD profile exhibits three distinct desorption peaks, a sharp peak at $T = 160$ K followed by a broad peak centered at $T = 206$ K, and a small peak at $T = 236$ K. The first peak is close to that of the pure diacetyl and is most likely due to diacetyl not trapped in the matrix, whereas the second peak represents different adsorption geometries within the acetaldehyde polymer matrix that are not notably occupied by diacetyl formed in the irradiation experiments. In contrast, the last peak appears at similar temperatures as seen

in the experiments only using acetaldehyde and is therefore likely linked to the adsorption site occupied by the diacetyl formed in the acetaldehyde irradiation experiments. This is further indicated by the overlap of this desorption event with that of the $C_4D_6O_2$ ($m/z = 92$) formed in the acetaldehyde- d_4 in this codeposition experiment.

The same delaying effect can be seen for the desorption of $C_5D_6H_3O_3$ at $m/z = 123$, which grows substantially upon irradiation and shifts from a peak sublimation temperature of $T = 155$ K in unprocessed ice to $T = 200$ K after irradiation as shown in Fig. S4. Based on TPD profiles (Fig. 5), their dependence on the photon energy (Fig. 6), and the FTIR data (Figs. 2-3), these findings concur with the formation of the diacetyl- d_6 isomer ($CD_3COCOCOD_3$; 92 amu) formed via recombination of two acetyl- d_3 ($CD_3\dot{C}O$) radicals. This conclusion seems to contradict the aforementioned predictions that the synthesis of three distinct isomers—diacetyl- d_6 , 2-oxobutanol- d_5 , and succinaldehyde- d_4 —has to be reflected by ion counts at three different m/z values of $m/z = 92$, 91 , and 90 . At 10.49 eV, the integrated signal strengths of $m/z = 90$ and $m/z = 91$ compared to $m/z = 92$ are $7 \pm 4\%$ and $21 \pm 5\%$, respectively.

Considering the isotopic purity of acetaldehyde-2,2,2- d_3 at the CD_3 group of $>98\%$, up to 6% of the acetaldehyde molecules could have one deuterium at the methyl group replaced by hydrogen. Therefore, as a result of the recombination of two acetyl- d_3 radicals ($CD_3\dot{C}O$), up to 12% of the formed molecules

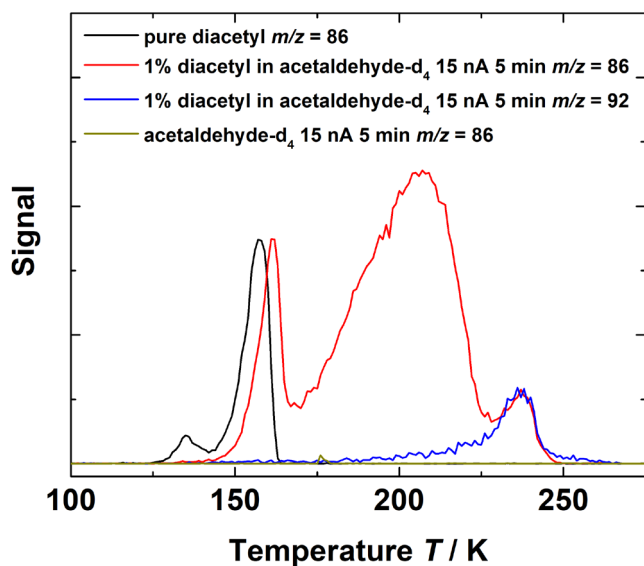


Figure 7. Temperature programmed desorption profiles of pure diacetyl, diacetyl added to acetaldehyde- d_4 and irradiated using the same parameters as in the other experiments and of the $C_4D_6O_2$ isomer formed from the irradiated acetaldehyde- d_4 . Desorption profiles were recorded at a photon energy of 10.49 eV.

could exhibit a mass-to-charge ratio of 91 and only 0.4% a mass-to-charge ratio of 90. These levels are too low to rationalize that ion counts at $m/z = 91$ and 90 are purely the results of the isotopic purity. This could either be explained by H/D exchange in the ice or alternative reaction mechanisms contributing to diacetyl- d_5 (91 amu) and diacetyl- d_4 (90 amu).

Detailed mechanistic studies with acetaldehyde-2,2,2- d_3 reveal that the dominating reaction pathway involves the unimolecular decomposition of acetaldehyde-2,2,2- d_3 via carbon-hydrogen single bond rupture forming atomic hydrogen along with the acetyl- d_3 radical ($CD_3\dot{C}O$). This process is endoergic by 377 kJ mol^{-1} (3.9 eV, Table S8, Supporting Information) with the energy for the bond cleavage supplied by the energetic electrons (reaction (1)). Two acetyl- d_3 radicals can recombine barrierlessly in an exoergic reaction (-303 kJ mol^{-1} ; 3.1 eV) to the diacetyl- d_6 isomer ($CD_3COC OCD_3$) if they have a favorable recombination geometry either at 5 K or at higher temperatures during the TPD phase, when they become more mobile inside the ice. The overall reaction to form diacetyl from two acetaldehyde molecules is endoergic by 451 kJ mol^{-1} (4.7 eV) and 14 kJ mol^{-1} (0.1 eV) for reaction (3) and (4) highlighting the need of *external* energy sources such as from galactic cosmic rays to convert acetaldehyde to diacetyl within extraterrestrial ices.

- (1) $2 \text{ CD}_3\text{CHO} \rightarrow 2 \text{ CD}_3\dot{\text{C}}\text{O} + 2 \text{ H}$
- (2) $\text{CD}_3\dot{\text{C}}\text{O} + \text{CD}_3\dot{\text{C}}\text{O} \rightarrow \text{CD}_3\text{COC OCD}_3$
- (3) $2 \text{ CD}_3\text{CHO} \rightarrow \text{CD}_3\text{COC OCD}_3 + 2 \text{ H}$
- (4) $2 \text{ CD}_3\text{CHO} \rightarrow \text{CD}_3\text{COC OCD}_3 + \text{H}_2$

The ion counts at $m/z = 91$ of diacetyl- d_5 detected at a level of $21 \pm 5\%$ compared to $m/z = 92$ would require a high level of H/D exchange to be rationalized with the aforementioned radical-radical recombination pathway (reactions (1)–(4)). Could the only other major reaction product—ketene- d_2 ($D_2\text{CCO}$)—play a role in the formation of diacetyl- d_5 ? As the formation of vinoxy- d_2 ($CD_2\dot{\text{C}}\text{HO}$) radicals is not observed in the FTIR spectra, the formation of ketene- d_2 does not proceed via hydrogen atom removal from the aldehyde group of the vinoxy- d_2 radical. Consequently, ketene- d_2 either forms by removal of one deuterium atom from the acetyl- d_3 radical by atomic hydrogen or by a concerted removal of the hydrogen atom from the aldehyde group and one deuterium atom from the methyl group leading to hydrogen deuteride (HD). This process is endoergic by 122 kJ mol^{-1} (1.3 eV), but this energy could be supplied by the impinging energetic electrons. Ketene- d_2 ($D_2\text{CCO}$) could react then with acetaldehyde- d_3 ($CD_3\text{CHO}$) via a concerted, four-center molecular reaction pathway leading to diacetyl- d_5 ($CHD_2\text{COC OCD}_3$). This reaction is exoergic by 107 kJ mol^{-1} (1.1 eV) but has to pass a transition state located about 170 kJ mol^{-1} (1.8 eV) above the separated reactants (reaction (5)). A comparison of this barrier to the endoergicity of the hydrogen atom loss from acetaldehyde forming the acetyl radical (reaction (1)) suggests that the barrier of the concerted, molecular reaction can be overcome with the excess energy supplied by the impinging radiation. Consequently, two pathways may contribute to the formation of diacetyl in acetaldehyde ices: a radical-radical mechanism leading to diacetyl- d_6 ($CD_3\text{COC OCD}_3$; 92 amu) and a molecular pathway forming diacetyl- d_5 ($CHD_2\text{COC OCD}_3$; 91 amu) with branching ratios defined by the ion counts of $m/z = 92$ and 91 detected of $4.8 \pm 1.0 : 1$. Most importantly, the detection of ketene- d_1 ($HD\text{CCO}$; 43 amu) at levels of $10 \pm 2\%$ with respect to ketene- d_2 ($D_2\text{CCO}$; 44 amu, Fig. 8) and inherent reaction with acetaldehyde- d_3 ($CD_3\text{CHO}$) to diacetyl- d_4 ($CH_2\text{DCOC OCD}_3$; 90 amu) involving the molecular pathways via reaction (6) might explain the detection of ion counts at $m/z = 90$ at levels of $7 \pm 4\%$ with respect to $m/z = 92$.

- (5) $D_2\text{CCO} + \text{CD}_3\text{CHO} \rightarrow \text{CHD}_2\text{COC OCD}_3$
- (6) $\text{HDCCO} + \text{CD}_3\text{CHO} \rightarrow \text{CH}_2\text{DCOC OCD}_3$

As acetaldehyde is only expected to be a minor constituent of interstellar ices with upper limits of 10 % with respect to water,^[5] the formation of diacetyl was additionally investigated in 10:1 mixtures of deuterium oxide (D_2O) and either acetaldehyde or acetaldehyde-2,2,2- d_3 . After subjecting these ices to 5 keV

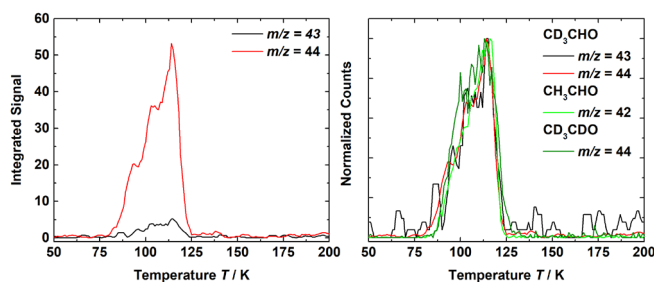


Figure 8. PI-ReToF-MS TPD profiles of ketene-d₂ ($m/z = 44$) and ketene-d₁ ($m/z = 43$) recorded at 10.11 eV after irradiation of acetaldehyde-2,2,2-d₃ ice (right) and normalized spectra compared to $m/z = 42$ and 44 in irradiated acetaldehyde and acetaldehyde-d₄, respectively, recorded at 10.49 eV

electrons with doses of 0.34 ± 0.05 eV molecule⁻¹, diacetyl was still detected as the main reaction product at $m/z = 86$ and $m/z = 92$ for acetaldehyde and acetaldehyde-2,2,2-d₃, respectively, as shown in Fig. 9 and Fig. S5. In these ice mixtures, the desorption profile of diacetyl exhibits two distinct events. The first desorption event coincides with the desorption of diacetyl not trapped in the polymer matrix (first peak in Fig. 7). By comparison with the desorption profile of deuterium oxide recorded by a quadrupole mass spectrometer, the second desorption peak can be attributed to codesorption of the diacetyl with the deuterium oxide, which is seen for most of the molecules present in the ice.

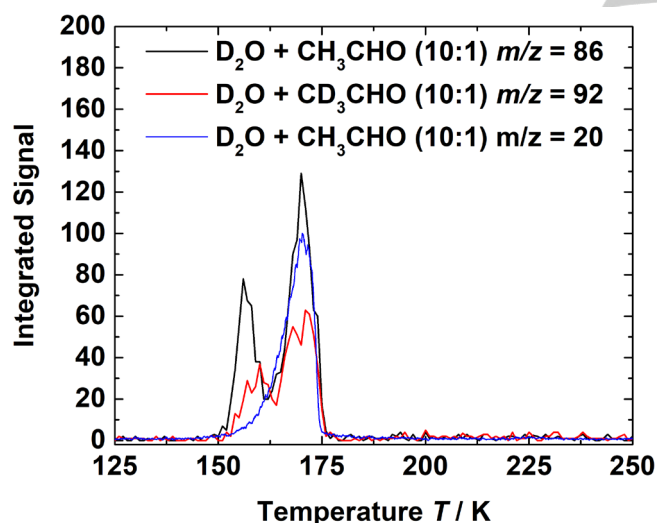


Figure 9. Temperature programmed desorption profiles of diacetyl ($m/z = 86$) formed in a 10:1 mixture of deuterium oxide and acetaldehyde and diacetyl-d₆ ($m/z = 92$) formed in a 10:1 mixture of deuterium oxide and acetaldehyde-d₃. The QMS signal for deuterium oxide ($m/z = 20$) is also shown to demonstrate the overlap of its desorption with the second desorption peak, indicating codesorption of the molecules.

Conclusion

To conclude, by exposing (partially deuterated) acetaldehyde interstellar analog ices to ionizing radiation and exploiting an array of complementary *in situ* analytical tools, the present study offers

compelling evidence on a facile formation of the diacetyl isomer ($\text{CH}_3\text{COCOCH}_3$). On Earth, the diacetyl molecule has been used to impart butter flavor in microwave popcorn and is also found in electronic cigarette fluids, where it is suspected to be linked to recent cases of vaping-related lung diseases^[72].

Overall, the identification of 2,3-butanedione (diacetyl)—a vicinal diketone carrying two adjacent C=O groups—provides convincing testimony that chemically complex organics carrying two carbonyl moieties can be synthesized easily in acetaldehyde-bearing interstellar and solar system ices either via a dominating radical-radical recombination pathway through acetyl radicals or through a molecular mechanism involving ketene and acetaldehyde with the excess energy for both mechanisms provided by the impinging energetic radiation. The reaction pathways leading to diacetyl are efficient enough to dominate the reactions even in a astrochemically more relevant 10:1 mixture of deuterium oxide and acetaldehyde. Therefore, 2,3-butanedione should be spectroscopically detectable upon sublimation of the irradiated ices in star forming regions as it has a non-zero dipole moment of about 1 Debye in the gas phase due to torsional vibration around the central C-C bond.^[73,74] With the commission of the Atacama Large Millimeter/Submillimeter Array (ALMA), the detection of heavier molecular weight organics will continue to grow, and a critical understanding of these data does rely on substantial advances in experimental laboratory astrophysics as demonstrated here.

Experimental Section

Experiments were conducted in an ultrahigh vacuum (UHV) chamber evacuated down to 10^{-11} Torr using hydrocarbon free magnetically levitated turbo molecular and scroll pumps.^[64] A silver mirror was mounted onto an oxygen free high conductivity copper target interfaced to a helium closed cycle refrigerator (cold head). Cooled down to 5 K, the cold head is rotatable and can be translated vertically using a doubly differentially pumped rotational feedthrough and a UHV compatible bellow. Isotopically labeled acetaldehyde (CD_3CDO , Sigma Aldrich, ≥ 99 atom % D; CD_3CHO , CDN isotopes, ≥ 98 atom % D) or unlabeled acetaldehyde (Sigma Aldrich, p. a., anhydrous, $\geq 99.5\%$ purity) was stored in a glass vial and residual atmospheric gases were removed by several freeze-thaw cycles exploiting liquid nitrogen. Acetaldehyde vapor was introduced into the main chamber through a glass capillary array at pressures of 3×10^{-8} Torr. The deposition onto the cooled silver substrate was monitored by recording interference fringes using a helium-neon laser (632.8 nm) and a photodiode as described previously.^[75] Using a

refractive index of $n = 1.303$ for acetaldehyde,^[76] the thickness of the ices was determined to be 500 ± 50 nm. After the deposition, an infrared spectrum was collected using a Fourier Transform Infrared (FTIR) spectrometer (Nicolet 6700). Afterwards, the ice was processed by irradiating an area of 1.0 ± 0.1 cm² with 5 keV electrons at a current of 15 ± 2 nA for 5 minutes (0.31 ± 0.06 eV molecule⁻¹) and 20 minutes (1.2 ± 0.2 eV molecule⁻¹) to simulate secondary electrons generated by galactic cosmic rays penetrating interstellar ices.^[77,78] Monte Carlo simulations were performed exploiting the CASINO program suite to determine the corresponding dose (Table S1).^[79] During the irradiation, IR spectra were collected to monitor the chemical changes *on line* and *in situ*. Following the irradiation, the temperature programmed desorption (TPD) phase was executed by heating the substrate from 5 K to 320 K at 0.5 K min⁻¹ thus subliming the acetaldehyde ice along with the volatile reaction products. Changes in the ice during the TPD were also monitored by taking IR spectra with integration times of 2 minutes to collect one spectrum per 1 K. This allows distinguishing between radicals, which will disappear at low temperatures due to their reactivity, and stable reaction products. Critical information on the nature of the subliming molecules is obtained by exploiting tunable vacuum ultraviolet (VUV) photoionization reflectron time-of-flight mass spectrometry (PI-ReToF-MS). The subliming molecules are ionized by coherent VUV light at 30 Hz repetition rate in a soft single photon ionization process to minimize (or exclude) fragmentation of parent molecules in the ionization process. The VUV light for this process was generated by resonant or non-resonant four wave mixing in a pulsed krypton or xenon gas jet with backing pressures of the pulsed valve at 2,000 Torr and pressures inside the mixing chamber around 10^{-4} Torr. Photon energies of 10.49 eV were generated inside the xenon jet by non-resonant four wave mixing of the frequency tripled output of a Nd:YAG laser (354.6 nm, Spectra Physics, Quanta Ray Pro 250-30). The remaining photon energies used in this study were generated by resonant four wave mixing^[80] in a xenon (10.11 eV, 9.50 eV) or krypton jet (9.30 eV, 9.10 eV). To achieve this, the outputs of two separate dye lasers (Sirah, Cobra-Stretch) pumped by two Nd:YAG lasers (Spectra Physics, Quanta Ray Pro 250-30 and 270-30, respectively) were tuned to the wavelengths needed to generate the VUV light and spatially and temporally overlapped inside the pulsed valve (Table S9, supporting information). Separation of different energies generated in the four-wave mixing was achieved by passing the beams through a bi-convex LiF lens in an off-axis geometry. The dispersion of this lens separates the different photon energies and allows only the desired photon energy to pass through a 1 mm aperture into the

main UHV chamber to ionize the molecules. The ions generated by the VUV light are then probed with a ReToF-MS (Jordan TOF Products, Inc.) and detected by a microchannel plate (MCP). A multichannel scalar (FAST ComTec, P788-1 E) analyzes the signal according to arrival times in 4 ns bin widths. Spectra are integrated for 3600 sweeps at 30 Hz, corresponding to an integration time of 2 minutes, which corresponds to a temperature increase in the TPD experiments of 1 K per individual mass spectrum.

Computational Methods

The geometries were optimized and harmonic frequencies computed utilizing density functional theory (DFT) via the B3LYP^[81–83] method along with the aug-cc-pVTZ basis set. These geometries are then utilized to determine single-point energies with coupled cluster theory at the singles, doubles, and perturbative triples [CCSD(T)] level^[84,85] in conjunction with aug-cc-pVTZ and aug-cc-pVQZ basis sets. The CCSD(T)/aug-cc-pVTZ and aug-cc-pVQZ energies are extrapolated to the complete basis set (CBS) limit via a 2-point formula.^[86] These CCSD(T)/CBS energies are then combined with the zero-point vibrational energies (ZPVEs) from B3LYP/aug-cc-pVTZ for the total energy of each isomer. The relative energies and ionization potentials are then determined from these CBS+ZPVE isomeric energies. The CCSD(T) computations utilize the Molpro2015.1 quantum chemistry program,^[87,88] and the DFT optimizations and vibrational frequencies are from Gaussian09.^[89]

Acknowledgements

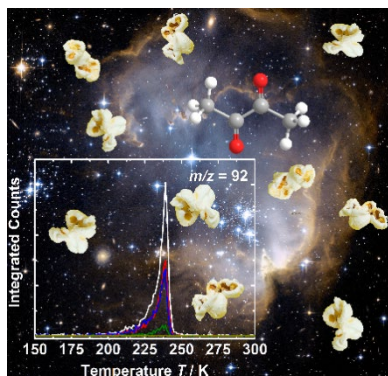
Financial support from the US National Science Foundation (AST-1800975) is greatly acknowledged (NFK, RIK). The experimental setup was financed by the W. M. Keck Foundation. The data analysis and preparation of the manuscript was partially supported by the Deutsche Forschungsgemeinschaft (DFG) (432686099; NFK). RCF acknowledges funding from NASA Grant NNX17AH15G and NSF Grant OIA-1757220, and he also wishes to thank C. Zachary Palmer of Georgia Southern University for assistance in generating the images utilized in Tables S5-S7 and Prof. Steven R. Davis for work related to exploring the transition states.

Keywords: complex organic molecules • interstellar synthesis • IR spectroscopy • mass spectroscopy • non-equilibrium processes

- [1] B. A. McGuire, *Astrophys. J. Suppl. Ser.* **2018**, *239*, 17.
- [2] E. Herbst, *Int. Rev. Phys. Chem.* **2017**, *36*, 287–331.
- [3] P. Ehrenfreund, S. B. Charnley, *Annu. Rev. Astron. Astrophys.* **2000**, *38*, 427–483.
- [4] A. C. A. Boogert, P. A. Gerakines, D. C. B. Whittet, *Annu. Rev. Astron. Astrophys.* **2015**, *53*, 541–581.
- [5] E. L. Gibb, D. C. B. Whittet, A. C. A. Boogert, A. G. G. M. Tielens, *Astrophys. J. Suppl. Ser.* **2004**, *151*, 35.
- [6] S. S. Prasad, S. P. Tarafdar, *ApJ* **1983**, *267*, 603–609.
- [7] M. H. Moore, R. L. Hudson, *Proc. Int. Astron. Union* **2005**, *1*, 247–260.
- [8] M. P. Bernstein, J. P. Dworkin, S. A. Sandford, G. W. Cooper, L. J. Allamandola, *Nature* **2002**, *416*, 401–403.
- [9] G. M. Muñoz Caro, U. J. Meierhenrich, W. A. Schutte, B. Barbier, A. Arcones Segovia, H. Rosenbauer, W. H.-P. Thiemann, A. Brack, J. M. Greenberg, *Nature* **2002**, *416*, 403–406.
- [10] P. de Marcellus, C. Meinert, M. Nuevo, J.-J. Filippi, G. Danger, D. Deboffe, L. Nahon, L. L. S. d'Hendecourt, U. J. Meierhenrich, *Astrophys. J.* **2011**, *727*, L27.
- [11] P. D. Holtom, C. J. Bennett, Y. Osamura, N. J. Mason, R. I. Kaiser, *Astrophys. J.* **2005**, *626*, 940–952.
- [12] R. I. Kaiser, A. M. Stockton, Y. S. Kim, E. C. Jensen, R. A. Mathies, *Astrophys. J.* **2013**, *765*, 111.
- [13] A. M. Turner, A. Bergantini, M. J. Abplanalp, C. Zhu, S. Góbi, B.-J. Sun, K.-H. Chao, A. H. H. Chang, C. Meinert, R. I. Kaiser, *Nat. Commun.* **2018**, *9*, 1–9.
- [14] A. M. Turner, M. J. Abplanalp, A. Bergantini, R. Frigge, C. Zhu, B.-J. Sun, C.-T. Hsiao, A. H. H. Chang, C. Meinert, R. I. Kaiser, *Sci. Adv.* **2019**, *5*, eaaw4307.
- [15] S. Maity, R. I. Kaiser, B. M. Jones, *Faraday Discuss.* **2014**, *168*, 485–516.
- [16] A. L. Weber, S. Pizzarello, *Proc. Natl. Acad. Sci. U. S. A.* **2006**, *103*, 12713–12717.
- [17] A. Strecker, *Justus Liebig's Ann. Chem.* **1850**, *75*, 27–45.
- [18] D. N. Simkus, J. C. Aponso, R. W. Hiltz, J. E. Elsil, C. D. K. Herd, *Meteorit. Planet. Sci.* **2019**, *54*, 142–156.
- [19] T. Butscher, F. Duvernay, G. Danger, T. Chiavassa, *Astron. Astrophys.* **2016**, *593*, A60.
- [20] C. J. Bennett, R. I. Kaiser, *Astrophys. J.* **2007**, *660*, 1289.
- [21] B. Marty, K. Altwegg, H. Balsiger, A. Bar-Nun, D. V. Bekaert, J.-J. Berthelier, A. Bieler, C. Briois, U. Calmonte, M. Combi, et al., *Science* **2017**, *356*, 1069–1072.
- [22] M. J. Mottl, B. T. Glazer, R. I. Kaiser, K. J. Meech, *Geochemistry* **2007**, *67*, 253–282.
- [23] A. M. Steer, N. Bia, D. K. Smith, P. A. Clarke, *Chem. Commun.* **2017**, *53*, 10362–10365.
- [24] C. J. Bennett, R. I. Kaiser, *Astrophys. J.* **2007**, *661*, 899–909.
- [25] C. J. Bennett, C. S. Jamieson, Y. Osamura, R. I. Kaiser, *Astrophys. J.* **2005**, *624*, 1097.
- [26] M. J. Abplanalp, S. Gozem, A. I. Krylov, C. N. Shingledecker, E. Herbst, R. I. Kaiser, *Proc. Natl. Acad. Sci.* **2016**, *113*, 7727–7732.
- [27] T. Lamberts, M. N. Markmeyer, F. J. Kolb, J. Kästner, *ACS Earth Space Chem.* **2019**, *3*, 958–963.
- [28] C. J. Bennett, Y. Osamura, M. D. Lebar, R. I. Kaiser, *Astrophys. J.* **2005**, *634*, 698.
- [29] S. Maity, R. I. Kaiser, B. M. Jones, *Phys. Chem. Chem. Phys.* **2015**, *17*, 3081–3114.
- [30] M. J. Abplanalp, R. I. Kaiser, *Phys. Chem. Chem. Phys.* **2019**, *21*, 16949–16980.
- [31] K. I. Öberg, R. T. Garrod, E. F. van Dishoeck, H. Linnartz, *Astron. Astrophys.* **2009**, *504*, 891–913.
- [32] R. Martín-Doménech, G. M. M. Caro, G. A. Cruz-Díaz, *Astron. Astrophys.* **2016**, *589*, A107.
- [33] R. L. Hudson, M. H. Moore, *Astrophys. J.* **2018**, *857*, 89.
- [34] H. E. Matthews, P. Friberg, W. M. Irvine, *Astrophys. J.* **1985**, *290*, 609–614.
- [35] N. Fourikis, M. W. Sinclair, B. J. Robinson, P. D. Godfrey, R. D. Brown, *Aust. J. Phys.* **1974**, *27*, 425–430.
- [36] A. Nummellin, J. E. Dickens, P. Bergman, A. Hjalmarson, W. M. Irvine, M. Ikeda, M. Ohishi, *Astron. Astrophys.* **1998**, *337*, 275–286.
- [37] B. E. Turner, R. Terzieva, E. Herbst, *Astrophys. J.* **1999**, *518*, 699–732.
- [38] G. A. Jungclaus, G. U. Yuen, C. B. Moore, J. G. Lawless, *Meteoritics* **1976**, *11*, 231–237.
- [39] J. Crovisier, D. Bockelée-Morvan, P. Colom, N. Biver, D. Despois, D. C. Lis, *Astron. Astrophys.* **2004**, *418*, 1141–1157.
- [40] K. Altwegg, H. Balsiger, J. J. Berthelier, A. Bieler, U. Calmonte, S. A. Fuselier, F. Goesmann, S. Gasc, T. I. Gombosi, L. Le Roy, et al., *Mon. Not. R. Astron. Soc.* **2017**, *469*, S130–S141.
- [41] W. A. Schutte, J. M. Greenberg, E. F. Van Dishoeck, A. G. G. M. Tielens, A. C. A. Boogert, D. C. B. Whittet, *Astrophys. Space Sci.* **1997**, *255*, 61–66.
- [42] W. A. Schutte, A. C. A. Boogert, A. G. G. M. Tielens, D. C. B. Whittet, P. A. Gerakines, J. E. Chiar, P. Ehrenfreund, J. M. Greenberg, E. F. van Dishoeck, Th. de Graauw, *Astron. Astrophys.* **1999**, *343*, 966–976.
- [43] A. G. Suits, *Acc. Chem. Res.* **2008**, *41*, 873–881.
- [44] K. J. Laidler, M. T. H. Liu, F. S. Dainton, *Proc. R. Soc. Lond. Ser. Math. Phys. Sci.* **1967**, *297*, 365–375.
- [45] A. K. Vasilou, K. M. Piech, B. Reed, X. Zhang, M. R. Nimlos, M. Ahmed, A. Golan, O. Kostko, D. L. Osborn, D. E. David, et al., *J. Chem. Phys.* **2012**, *137*, 164308.
- [46] L. B. Harding, Y. Georgievskii, S. J. Klippenstein, *J. Phys. Chem. A* **2010**, *114*, 765–777.
- [47] R. Sivaramakrishnan, J. V. Michael, L. B. Harding, S. J. Klippenstein, *J. Phys. Chem. A* **2015**, *119*, 7724–7733.
- [48] A. Horowitz, C. J. Kershner, J. G. Calvert, *J. Phys. Chem.* **1982**, *86*, 3094–3105.
- [49] H.-K. Li, P.-Y. Tsai, K.-C. Hung, T. Kasai, K.-C. Lin, *J. Chem. Phys.* **2015**, *142*, 041101.
- [50] B. R. Heazlewood, M. J. T. Jordan, S. H. Kable, T. M. Selby, D. L. Osborn, B. C. Shepler, B. J. Braams, J. M. Bowman, *Proc. Natl. Acad. Sci.* **2008**, *105*, 12719–12724.
- [51] K. L. K. Lee, M. S. Quinn, A. T. Maccarone, K. Nauta, P. L. Houston, S. A. Reid, M. J. T. Jordan, S. H. Kable, *Chem. Sci.* **2014**, *5*, 4633–4638.
- [52] K. M. Kapnas, L. M. McCaslin, C. Murray, *Phys. Chem. Chem. Phys.* **2019**, *21*, 14214–14225.
- [53] Y.-C. Han, P.-Y. Tsai, J. M. Bowman, K.-C. Lin, *Phys. Chem. Chem. Phys.* **2017**, *19*, 18628–18634.
- [54] K.-C. Hung, P.-Y. Tsai, H.-K. Li, K.-C. Lin, *J. Chem. Phys.* **2014**, *140*, 064313.
- [55] T. Y. Kang, S. W. Kang, H. L. Kim, *Chem. Phys. Lett.* **2007**, *434*, 6–10.
- [56] S.-H. Lee, *J. Chem. Phys.* **2009**, *131*, 174312.
- [57] A. W. Harrison, A. Kharazmi, M. F. Shaw, M. S. Quinn, K. L. K. Lee, K. Nauta, K. N. Rowell, M. J. T. Jordan, S. H. Kable, *Phys. Chem. Chem. Phys.* **2019**, *21*, 14284–14295.
- [58] P. Swiderek, C. Jäggle, D. Bankmann, E. Burean, *J. Phys. Chem. C* **2007**, *111*, 303–311.
- [59] V. I. Feldman, F. F. Sukhov, A. Yu. Orlov, N. A. Shmakova, *High Energy Chem.* **2001**, *35*, 319–327.
- [60] V. Belevskii, S. Belopushkin, V. Feldman, *J. Radioanal. Nucl. Chem.* **1985**, *96*, 137–151.
- [61] C. Chaechaty, R. Marx, *J. Chim. Phys.* **1961**, *58*, 787–789.
- [62] S. E. Bisschop, G. W. Fuchs, E. F. van Dishoeck, H. Linnartz, *Astron. Astrophys.* **2007**, *474*, 1061–1071.
- [63] R. L. Hudson, R. F. Ferrante, *Mon. Not. R. Astron. Soc.* **2020**, *492*, 283–293.
- [64] B. M. Jones, R. I. Kaiser, *J. Phys. Chem. Lett.* **2013**, *4*, 1965–1971.
- [65] M. J. Abplanalp, S. Góbi, R. I. Kaiser, *Phys. Chem. Chem. Phys.* **2019**, *21*, 5378–5393.
- [66] K. I. Öberg, A. C. A. Boogert, K. M. Pontoppidan, S. van den Broek, E. F. van Dishoeck, S. Bottinelli, G. A. Blake, N. J. Evans, *Proc. Int. Astron. Union* **2011**, *7*, 65–78.
- [67] G. J. Jiang, W. B. Person, K. G. Brown, *J. Chem. Phys.* **1975**, *62*, 1201–1211.
- [68] R. L. Hudson, M. J. Loeffler, *Astrophys. J.* **2013**, *773*, 109.
- [69] M. E. Jacox, *Chem. Phys.* **1982**, *69*, 407–422.
- [70] M. J. Abplanalp, S. Góbi, A. Bergantini, A. M. Turner, R. I. Kaiser, *ChemPhysChem* **2018**, *19*, 556–560.
- [71] A. Charlesby, *Rep. Prog. Phys.* **1965**, *28*, 463–518.
- [72] S. T. Landman, I. Dhaliwal, C. A. Mackenzie, T. Martinu, A. Steele, K. J. Bosma, *CMAJ* **2019**, *191*, E1321–E1331.
- [73] A. Gómez-Zavaglia, R. Fausto, *J. Mol. Struct.* **2003**, *661–662*, 195–208.
- [74] G. I. M. Bloom, L. E. Sutton, *J. Chem. Soc.* **1941**, 727–742.
- [75] A. M. Turner, M. J. Abplanalp, S. Y. Chen, Y. T. Chen, A. H. H. Chang, R. I. Kaiser, *Phys. Chem. Chem. Phys.* **2015**, *17*, 27281–27291.
- [76] R. L. Hudson, F. M. Coleman, *Phys. Chem. Chem. Phys.* **2019**, *21*, 11284–11289.
- [77] R. I. Kaiser, K. Roessler, *Astrophys. J.* **1997**, *475*, 144.
- [78] R. I. Kaiser, G. Eich, A. Gabrysch, K. Roessler, *Astrophys. J.* **1997**, *484*, 487.
- [79] D. Drouin, A. R. Couture, D. Joly, X. Tastet, V. Aimez, R. Gauvin, *Scanning* **2007**, *29*, 92–101.
- [80] R. Hilbig, R. Wallenstein, *IEEE J. Quantum Electron.* **1981**, *17*, 1566–1573.
- [81] W. Yang, R. G. Parr, C. Lee, *Phys. Rev. A* **1986**, *34*, 4586–4590.
- [82] C. Lee, W. Yang, R. G. Parr, *Phys. Rev. B* **1988**, *37*, 785–789.
- [83] A. D. Becke, *J. Chem. Phys.* **1993**, *98*, 5648–5652.
- [84] T. D. Crawford, H. F. Schaefer III, in *Rev. Comput. Chem.*, John Wiley & Sons, Ltd, **2000**, pp. 33–136.
- [85] K. Raghavachari, G. W. Trucks, J. A. Pople, M. Head-Gordon, *Chem. Phys. Lett.* **1989**, *157*, 479–483.
- [86] S. B. Huh, J. S. Lee, *J. Chem. Phys.* **2003**, *118*, 3035–3042.
- [87] H.-J. Werner, P. J. Knowles, G. Knizia, F. R. Manby, M. Schütz, *WIREs Comput Mol Sci* **2012**, *2*, 242–253.
- [88] H.-J. Werner, P. J. Knowles, G. Knizia, F. R. Manby, M. Schütz, others, *MOLPRO, Version 2015.1, a Package of Ab Initio Programs*, Cardiff, UK, **2015**.

- [89] M. J. Frisch, G. W. Trucks, H. B. Schlegel, G. E. Scuseria, M. A. Robb, J. R. Cheeseman, G. Scalmani, V. Barone, G. A. Petersson, H. Nakatsuji, et al., *Gaussian 09 Revision D.01*, Gaussian Inc., Wallingford, CT, **2009**.

Entry for the Table of Contents



Exploiting photoionization reflectron time-of-flight mass spectrometry, we demonstrate that the popcorn and butter flavorant 2,3-butanedione (diacetyl) represents the main reaction product of acetaldehyde ices exposed to ionizing radiation.

Institute and/or researcher Twitter usernames: @UHMRxnDynamics